

STRANGENESS PHYSICS WITH CLAS AT JLAB

Volker D. Burkert

Jefferson Lab, Newport News, VA 23606, USA

**E-mail: burkert@jlab.org*

A brief overview of strangeness physics with the CLAS detector at JLab is given, mainly covering the domain of nucleon resonances. Several excited states predicted by the symmetric constituent quark model may have significant couplings to the $K\Lambda$ or $K\Sigma$ channels. I will discuss data that are relevant in the search for such states in the strangeness channel, and give an outlook on the future prospects of the N^* program at JLab with electromagnetic probes.

Keywords: Hyperons, complete experiments, missing resonances

1. Introduction

A major goal of hadron physics with electromagnetic probes is to study the structure of the nucleon and its excited states. The nucleon excitation spectrum is a direct reflection of the underlying degrees of freedom. For example, the $SU(6)$ symmetric constituent quark model predicts a large number of states many of which have not been observed experimentally using hadronic probes. A model that includes clustering of two quarks into di-quarks has fewer degrees of freedom and predicts a smaller number of excited states. It is obviously important to obtain a better understanding of the degrees of freedom underlying the nucleon properties. Most studies of the nucleon spectrum have used pion probes. Electromagnetic probes, photons and electrons, and strangeness production are complementary ways to search for some of the excited states and can help discriminate between alternative description of the nucleon spectrum. The CLAS program is designed to accurately measure electromagnetic cross sections and single and double polarization observables with wide energy and angle coverage.

2. Experimental aspects

The experimental program makes use of the CEBAF Large Acceptance Spectrometer (CLAS) ¹ which provides particle identification and momen-

tum analysis in a polar angle range from 8° to 140° . The photon energy tagger provides energy-marked photons with an energy resolution of $\frac{\sigma(E)}{E} = 10^{-3}$. Other equipment includes a coherent bremsstrahlung facility with a goniometer for diamond crystal positioning and angle control. The facility has been used for linearly polarized photons with polarizations up to 90%. There are two frozen spin polarized targets, one based on butanol as target material (FROST), and one using HD as a target material (HD-Ice). The latter is currently under construction. FROST has already been operated successfully in longitudinal polarization mode and will be used in transverse polarization mode in 2010. HD-Ice will be used as polarized neu-

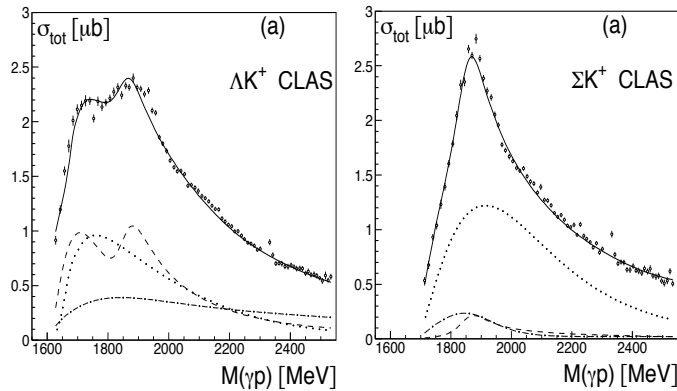


Fig. 1. Integrated total cross section data for $K^+\Lambda$ and $K^+\Sigma^0$ channels. The lines represent the fit results of the Bonn-Gatchina coupled-channel analysis. The dashed line shows the energy-dependence of the P_{13} partial wave which indicates the presence of two P_{13} resonances at 1720 MeV and at 1900 MeV, respectively. The new $P_{13}(1900)$ contributes a significant fraction to the total $K^+\Lambda$ cross section.

tron (deuteron) target in 2010/2011. Circularly polarized photons can be generated by scattering the highly polarized electron beam from an amorphous radiator. It is well understood that measurements of differential cross sections in photoproduction of single pseudoscalar mesons alone results in ambiguous solutions for the contributing resonant partial waves. The N^*

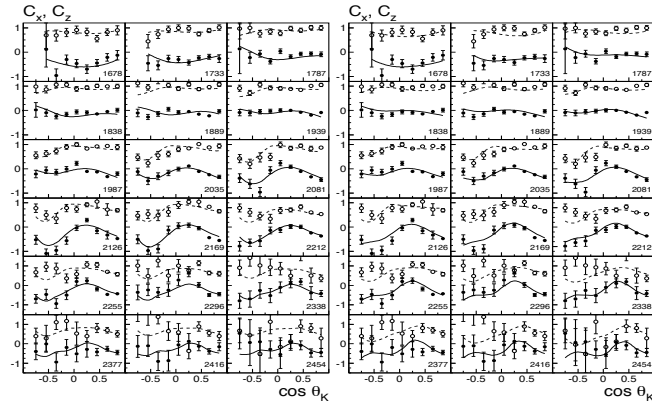


Fig. 2. Angular dependence of polarization transfer observables $C_{x'}$, C_z . The panel on the left and right show different solutions of the Bonn-Gatchina fit. A $P_{13}(1900)$ resonance is needed to obtain a good fit.

program at JLab is therefore aimed at complete, or nearly complete measurements for processes $\vec{\gamma}\vec{p} \rightarrow \pi N$, ηp , $K^+\vec{Y}$ and $\vec{\gamma}\vec{n} \rightarrow \pi N$, $K\vec{Y}$. Complete information can be obtained by using a combination of linearly and circularly polarized photon beams, measurement of hyperon recoil polarization, and the use targets with longitudinal and transverse polarization. The reaction is fully described by 4 complex parity conserving amplitudes, requiring 8 combinations of beam, target, and recoil polarization measurements for an unambiguous extraction of the scattering amplitude. If all possible combinations are measured, 16 observables can be extracted. In measurements that involve nucleons in the final state where the recoil polarization is not measured, 7 independent observables can be obtained directly, and the recoil polarization asymmetry P can be inferred from the double polarization asymmetry with linearly polarized beam and transverse target polarization.

3. Search for N^* states in KY channels

A large amount of cross section data have been collected in recent years on the $K\Lambda$ and $K\Sigma$ photo-production.^{2,3} These data cover the nucleon resonance region in fine steps of about 10 MeV in the hadronic mass W , and nearly the entire polar angle range. The integrated cross section shown in Fig. 1 reveals a strong bump around $W = 1900$ MeV which may be the result of s-channel resonance production. However, more definite conclusions can only be drawn when polarization observables are included in the analysis. First differential cross sections of the channel $\gamma p \rightarrow K^{*\circ}\Sigma^+$, which probes the mass range $W > 2100$ MeV have been measured recently,⁵ and will be continued at higher statistics.

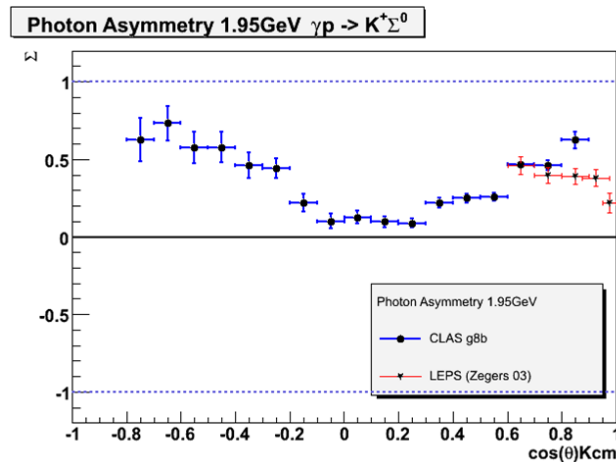


Fig. 3. Preliminary data from CLAS for the beam asymmetry of the $K\Sigma^0$ final state.

3.1. Polarized beam and spin transfer

Fitting differential cross sections alone has not resulted in unambiguous identification of a specific s-channel resonance. In addition to precise $K\Lambda$ and $K\Sigma$ cross section data, recoil polarization and polarization transfer data have been measured.⁴ The recoil polarization data in the $K^+\Lambda$ sector showed a highly unexpected behavior: The spin transfer from the circularly polarized photon to the Λ hyperon is complete, leaving the Λ hyperon 100% polarized, as can be seen in Fig. 4. The sum of all polarization components

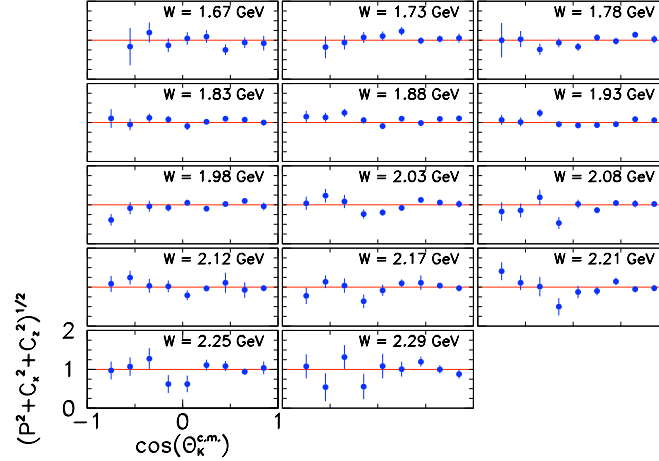


Fig. 4. Spin transfer from the polarized photon to the final state Λ . The spin transfer data were fitted by the Bonn-Gatchina group simultaneously with the CLAS $K^+\Lambda$ and $K^+\Sigma$ differential cross section data. A $P_{13}(1900)$ state is required for the best fit to the cross section and spin transfer data.

$R^2 \equiv P^2 + C_x^2 + C_z^2$ which has an upper bound of 1, is consistent with $R^2 = 1$ throughout the region covered by measurement. At first glance this result seems adverse to the idea that the $K\Lambda$ final state has a significant component of N^* resonance associated with. However, the analysis of the combined CLAS differential cross section and polarization transfer data by the Bonn-Gatchina group⁶ shows strong sensitivity to a $P_{13}(1900)$ candidate state. The decisive ingredient in this analysis is the CLAS spin transfer data set. We remark that the peak observed in the $K^+\Lambda$ data seen near 1900 MeV in Fig. 2 was originally attributed to a $D_{13}(1900)$ resonance before the spin transfer data became available. A $P_{13}(1900)$ is listed as a 2-star candidate state in the 2008 edition of the RPP.⁷ If this assignment is confirmed in future analyses which should include additional polarization data, the existence of a $P_{13}(1900)$ state would be strong evidence against the quark-diquark model. This model has no place for such a state in this mass range.⁸ New precise high statistics data with linearly polarized photon beam on proton targets have also become available. Preliminary results for the process $\gamma p \rightarrow K^+\Sigma^0$ are shown for a single energy bin in Fig. 3. Eventually, these data will span the resonance mass region up to $W = 2.5$ GeV. Several other strangeness channels such as $\gamma n \rightarrow K^0\Lambda$, $K^{*0}\Lambda$, $K^0\Sigma^0$, $K^+\Sigma^-$, and

$K^+\Sigma^-(1385)$ are currently being investigated to search for new states on neutron targets using circularly and linearly polarized photon beams. For most of these channel a complete kinematical reconstruction in the neutron rest frame is possible, thus eliminating the effect of Fermi motion in the deuteron nucleus. Recoil polarization measurements in all hyperon final states are also available for the analysis.

4. Search for new cascade baryons

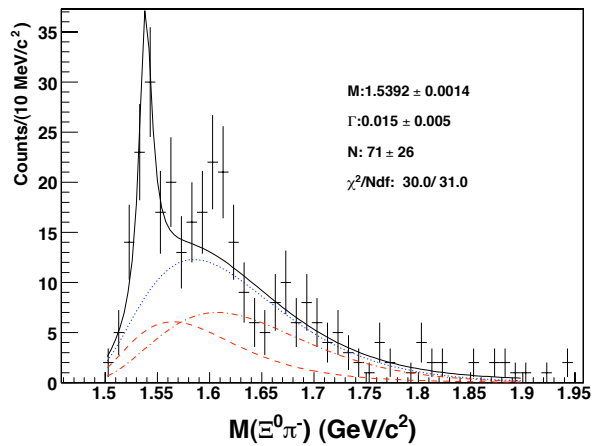


Fig. 5. Mass of the $\Xi\pi^-$ final state. The $\Xi(1530)$ is clearly seen. A structure near 1620 MeV could be related to a dynamically generated Ξ state predicted in the model of Ref.⁹

The production of Ξ hyperons, i.e. strangeness $S = -2$ excited states, presents another promising way of searching for new baryon states. The advantages of cascade hyperon states are due to the expected narrow widths of these states compared to $S = 0$, and $S = -1$ resonances. The disadvantages of using photon beams are also obvious: The $S = -2$ requires production of at least two kaons in the final state. Possible production mechanisms include t-channel K or K^* exchanges on proton targets with an excited hyperon Y^* (Λ^* or Σ^*) as intermediate state and subsequent decays $Y^* \rightarrow K^+\Xi^*$ and $\Xi^* \rightarrow \Xi\pi$ or $\Xi \rightarrow \Lambda(\Sigma)\bar{K}$. Missing mass technique may be used to search for new states in the reaction $\gamma p \rightarrow K^+K^+X$ if the state is sufficiently narrow to be observed as a peak in the missing mass

spectrum. However, an analysis of the final state is needed to assign spin and parity to the state. Data from CLAS taken at 3.6 GeV beam energy show that one can identify the lowest two cascade states this way.¹⁰ To identify the higher mass states higher energy is needed. Another approach

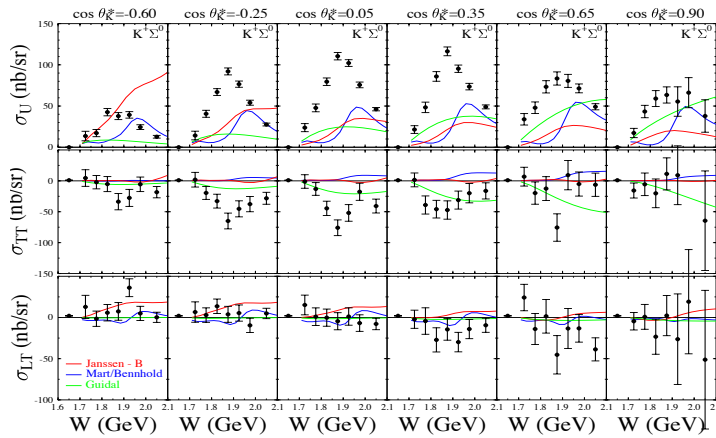


Fig. 6. Separated response functions for $K^+\Sigma^0$ electroproduction. The response function σ_u and σ_{TT} show strong resonance-like structure near $W = 1.9\text{GeV}$, which is not reproduced by any model.

to isolate excited cascades and determine their spin-parity, is to measure additional particles in the final state. The invariant mass of the $\Xi\pi^-$ system is displayed in Fig. 5 and shows the first excited state $\Xi(1530)$ and indications of additional structure near 1620 MeV. A state near that mass is predicted⁹ as a dynamically generated $\Xi\pi$ system. The data have insufficient statistics and were taken at too low energy to allow further investigations. New data taken at 5.7 GeV electron energy and with higher statistics are currently being analyzed, and should allow more definite conclusions on a possible new Ξ state at that mass.

5. Strangeness electroproduction

Significant effort has been devoted to the study of electroproduction of hyperons^{11,12} as a complementary means of searching for new excited nucleon states. Figure 6 shows the dependence of the response functions on the hadronic mass W . The comparison with model calculations reveals large discrepancies. None of the models that include known nucleon resonance

couplings to $K\Sigma$, is able to get the normalization correct. This leaves much room for yet to be identified resonance strength.

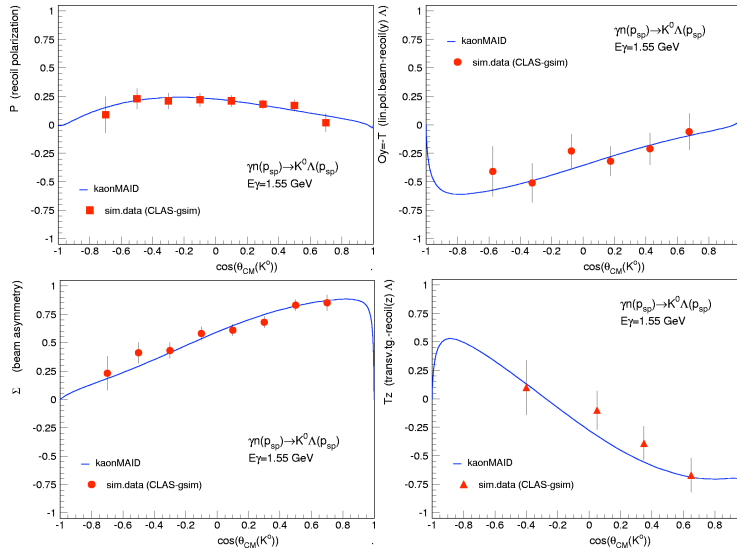


Fig. 7. Data samples for the process $\gamma n \rightarrow K_s^0 \vec{\Lambda}$ projected for the upcoming polarized target run using the HD-Ice facility at JLab.

6. Outlook

The power of polarization measurements for the resonance analysis will be brought to bear when double and triple polarization data are available making use of longitudinally and transversely polarized proton and neutron targets. Data with the polarized proton target (FROST) combined with linearly and circularly polarized photons are currently in the analysis stage. Measurements with transverse polarized proton targets are planned for 2010.

Measurement of polarization observables using polarized neutrons are planned for 2010/2011. Some projected data using the HD-Ice target facility in the CLAS detector are shown in Fig. 7. Single polarization observables P , Σ and double polarization asymmetries for beam-recoil polarization $O_{y'}$,

and target-recoil polarization $T_{z'}$, are shown. Other observables, e.g. target asymmetry T , beam-target asymmetries E , F , and G , H will be measured as well. The projections are for one photon energy bin out of over 25 bins. The solid line is the projection of the kaonMAID code.¹³

Authored by The Southeastern Universities Research Association, Inc. under U.S. DOE Contract No. DE-AC05-84ER40150 . The U.S. Government retains a non-exclusive, paid-up, irrevocable, world-wide license to publish or reproduce this manuscript for U.S. Government purposes.

References

1. B. Mecking et al., *Nucl. Instrum. Meth.* **A503**, 513 , 2003.
2. R. Bradford et al., (CLAS Collaboration), *Phys. Rev.* **C73**, 035202, 2006.
3. J. W. McNabb et al., (CLAS Collaboration), *Phys. Rev.* **C69** 042201, 2004.
4. R. Bradford et al., (CLAS Collaboration), *Phys. Rev.* **C75**, 035205, 2007.
5. I. Hleiqawi et al., (CLAS Collaboration), *Phys. Rev.* **C75**, 042201, 2007, Erratum-ibid.C76:039905,2007.
6. V.A. Nikonov et al., *Phys. Lett.* **B662**, 245, 2008.
7. C. Amsler et al., *Phys. Lett.* **B667**, 1, 2008.
8. E. Santopinto, *Phys. Rev.* **C72**, 022201, 2005.
9. A. Ramos, E. Oset, C. Bennhold, *Phys.Rev.Lett.***89**:252001,2002.
10. L. Guo et al., (CLAS Collaboration), *Phys. Rev.* **C76**, 025208, 2007.
11. P. Ambrozewicz et al. (CLAS Collaboration), *Phys. Rev.* **C75**, 045203, 2007.
12. D. Carman et al., (CLAS Collaboration), *arXiv*:0904.3246, 2009.
13. F.X. Lee, T. Mart, C. Bennhold, H. Haberzettl, L.E. Wright, *Nucl. Phys.* **A695** (2001) 237